MUSCULOSKELETAL

Bone marrow edema in non-traumatic hip: high accuracy of dual-energy CT with water-hydroxyapatite decomposition imaging

Wookon Son[1] · Chankue Park[1] · Hee Seok Jeong[1] · You Seon Song[2] · In Sook Lee[2]

Abstract

Objectives To evaluate the diagnostic performance of dual-energy CT with water-hydroxyapatite (HAP) imaging for bone marrow edema in patients with non-traumatic hip pain.

Methods Forty patients (mean age, 58 years; 16 male and 24 female) who underwent rapid kVp-switching dual-energy CT and MRI within 1 month between April 2018 and February 2019 with hip pain but no trauma were enrolled. Two radiologists retrospectively evaluated 80 hip joints for the presence, extent (femoral head involved, head and neck, and head to intertrochanter), and severity (mild edema, moderate, severe) of bone marrow edema on dual-energy water-HAP images. Water mass density (mg/cm^3) on water-HAP images was determined with region of interest–based quantitative analysis. MRI served as the standard of reference.

Results Sensitivity, specificity, and accuracy of readers 1 and 2 for the identification of bone marrow edema in water-HAP images were 85% and 85%, 93% and 73%, and 89% and 79%, respectively. The area under the receiver operating characteristic curve was 0.96 for reader 1 and 0.91 for reader 2 for differentiation of the presence of edema from no edema. The optimal water mass density to classify the presence of edema for reader 1 was 951 mg/cm^3 with 93% sensitivity and 93% specificity and for reader 2 was 957 mg/cm^3 with 80% sensitivity and 80% specificity. The more severe the edema, the higher was the mean water density value ($p < 0.035$).

Conclusion Dual-energy water-HAP images showed good diagnostic performance for bone marrow edema in patients with non-traumatic hip pain.

Key Points

• *Dual-energy water-HAP imaging depicts bone marrow edema in patients with non-traumatic hip pain and may serve as an alternative to MRI in select patients.*

• *A cutoff value of 951 mg/cm^3 mean water mass density results in 93% sensitivity and 93% specificity for the detection of bone marrow edema.*

• *The more severe the bone marrow edema, the higher the mean water density value.*

Keywords Bone marrow · Edema · Hip joint · Dual-energy scanned projection radiography · X-ray computed tomography

Abbreviations

AUROC	Area under the receiver operating characteristic
CI	Confidence interval
CT	Computed tomography
CTDI	Computed tomography dose index
DECT	Dual-energy computed tomography
HAP	Hydroxyapatite
ICC	Interclass correlation coefficient
MR	Magnetic resonance
MRI	Magnetic resonance imaging
NPV	Negative predictive value
PPV	Positive predictive value
ROC	Receiver operating characteristic
ROI	Region of interest

✉ Chankue Park
chankue.park@gmail.com

1 Department of Radiology, Pusan National University Yangsan Hospital, 20, Geumo-ro, Mulgeum-eup, Yangsan-si, Gyeongsangnam-do, Korea

2 Department of Radiology, Pusan National University Hospital, Busan, Korea

Introduction

Hip osteoarthritis and osteonecrosis are common causes of non-traumatic hip pain in adults [1, 2]. In osteoarthritis, bone marrow edema is associated with higher grades of articular cartilage defects, severity of hip pain, and radiographic grading, and it is a potent risk factor for structural deterioration [3–5]. In osteonecrosis, bone marrow edema is correlated with necrotic volume and is the most significant risk factor for worsening of hip pain and a marker for potential progression to advanced osteonecrosis [6, 7]. Bone marrow edema also affects hip pain in other non-traumatic hip diseases, including inflammatory arthropathy, transient osteopenia, infection, and tumors [8].

Although magnetic resonance imaging (MRI) is the usual diagnostic imaging modality for depicting bone marrow edema, it is more time consuming and expensive than other modalities [9–12]. Patients with pacemakers, cochlear implants, claustrophobia, or who are unable to lie down for long periods are limited for MRI. Conventional computed tomography (CT) is a good modality to evaluate structural abnormalities of bone, with relatively shorter examination times and lower costs than MRI [9, 13]. However, it is difficult to evaluate bone marrow edema on conventional CT [14, 15].

Dual-energy CT (DECT) allows the identification of bone marrow edema by subtracting the signal from the bone mineral matrix based on material-specific attenuation at different X-ray energies [16–18]. Virtual non-calcium images by three-material decomposition showed good diagnostic performance in evaluating traumatic bone marrow edema, plasma cell infiltration, and bone marrow edema of sacroiliitis in axial spondyloarthritis [11, 12, 14–16, 19–21]. One study [22] showed the possibility of detecting bone marrow edema in vertebral compression fractures on DECT material density imaging with two-material decomposition between water and calcium. Material density images with two-material decomposition assume the entire volume which comprises only two pre-selected materials. Any two materials can be selected for two-material DECT decomposition, depending on the clinical purpose [17]. In this study, we selected water and hydroxyapatite (HAP) as materials for material decomposition as human bones consist of 50% organic matrix (osteoid) and 50% calcium HAP [23, 24].

We aimed to evaluate the diagnostic performance of DECT with water-HAP density imaging in detecting bone marrow edema in patients with non-traumatic hips.

Materials and methods

This retrospective study was approved by the institutional review board and the need for informed consent was waived.

Study population

Three hundred and fifty-four adult patients had hip CT examinations at our institution from April 2018 to February 2019. Of those 354 patients, 95 patients underwent DECT. Forty-three of these patients had DECT and MRI within 1 month. Of those 43 patients, 3 patients who underwent hip replacement arthroplasty were excluded. The remaining 40 patients had hip pain, but no history of recent trauma within 3 months. Ai et al reported that no bone marrow edema was identified on DECT images performed after 11 weeks following injury [25]. Our final study group consisted of 40 patients (80 hip joints) with non-traumatic hip pain who had DECT and MRI within 1 month (Fig. 1).

Information regarding age, gender, hip symptom, clinical diagnosis, and CT and MR examination date was obtained from medical records.

DECT scan protocol and material density image reconstruction

All patients studied were examined with third-generation 256-slice DECT (Revolution CT; GE Healthcare). Our routine hip DECT protocol consists of conventional imaging with axial, sagittal, and coronal views and water-HAP imaging with axial and coronal views. However, we evaluated only the water-HAP images in this study. The scan protocols were as follows: single-source rapid kVp-switching dual-energy scan with 80 and 140 kVp; manual tube current setting, 405 mA; helical pitch, 0.508; table speed, 67.71 mm/s; and rotation time, 0.6 s/rotation. The mean volume CT dose index (CTDI) was 11.1 mGy (95% confidence interval [CI], 10.4, 11.9 mGy; range, 10.4–19.9 mGy) and the mean dose-length product was 390.7 mGy cm (95% CI, 358.6, 422.8 mGy cm; range, 322.9–778.9 mGy cm). No intravenous contrast agent was administered.
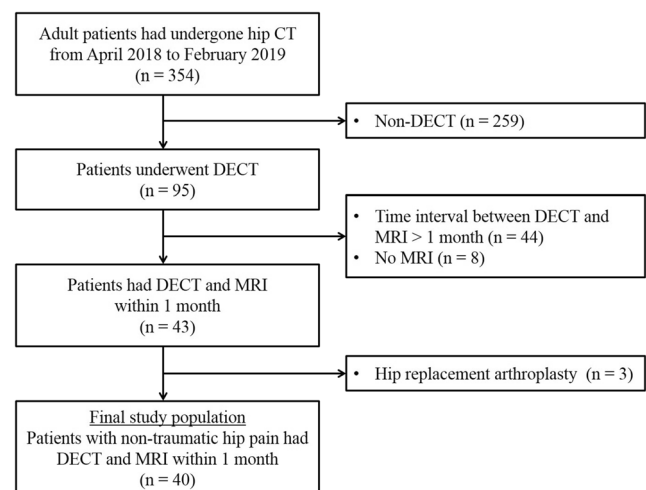

Fig. 1 Flow diagram of the study patients. *DECT*, dual-energy CT

Low- and high-energy sinograms were acquired by rapid kVp-switching using a single X-ray tube [17]. Using two-material decomposition algorithm, the low- and high-kilovolt projections were transformed into material density images of each material.

The two-material decomposition algorithm assumes that the entire volume is made of only two materials: in this case, water and HAP. The material densities of water and HAP in each voxel are calculated by the following process. The linear attenuation coefficient, μ_L, is expressed as the linear equation system [18],

$$\mu_L(E_{\text{low}}) = \rho_W \cdot \mu_{M,W}(E_{\text{low}}) + \rho_H \cdot \mu_{M,H}(E_{\text{low}}) \qquad (1)$$

$$\mu_L(E_{\text{high}}) = \rho_W \cdot \mu_{M,W}(E_{\text{high}}) + \rho_H \cdot \mu_{M,H}(E_{\text{high}}) \qquad (2)$$

where $\mu_L(E)$ is measured at the distinct energy levels E_{low} and E_{high}; ρ_w and ρ_H are the material densities of water and HAP, respectively; and $\mu_{M,\,W}(E)$ and $\mu_{M,\,H}(E)$ are the mass attenuation coefficients of water and HAP at energy E. The mass attenuation coefficients were obtained from standardized tables [26, 27].

Water-HAP images illustrate water density with suppressed HAP information. Measured pixel intensity value in the material density images corresponds to material density and is expressed as mg/cm^3. Axial and coronal grayscale water-HAP images were generated with a 2.5-mm section thickness by using a standard kernel including adaptive statistical iterative reconstruction-V (GE Healthcare), 40% standard. All reconstructed images were automatically transferred to a picture archiving and communication system.

MRI protocol

All MRI examinations were performed using a 3.0-T unit (Magnetom Skyra; Siemens Healthineers) in 24 patients and a 1.5-T MR unit (Magnetom Avanto; Siemens Healthineers) in 16 patients with phased-array surface coil. The hip MRI consisted of axial, coronal, and sagittal T1- and fat-suppressed T2-weighted fast spin-echo sequences. However, we evaluated only the axial and coronal T1- and fat-suppressed T2-weighted images. The 3.0T MR protocols are an axial T1-weighted sequence (repetition time ms/echo time ms, 542/9; echo train length, 3; matrix, 512 × 374) and an axial fat-suppressed T2-weighted sequence (3190/90; echo train length, 14; matrix, 448 × 402), with a 3-mm section thickness, 0.3-mm intersection gap, and 384 × 300 mm field of view; and a coronal T1-weighted sequence (542/9; echo train length, 3; matrix, 512 × 374) and a coronal fat-suppressed T2-weighted sequence (3060/80; echo train length, 14; matrix, 512 × 312), with a 3-mm section thickness, 0.3-mm intersection gap, and 380 × 389 mm field of view. The 1.5-T MR protocols are an axial T1-weighted sequence (547/21; echo train length, 21; matrix, 384 × 176) and an axial fat-

suppressed T2-weighted sequence (3000/72; echo train length, 10; matrix, 350 × 228), with a 3-mm section thickness, 1.2-mm intersection gap, and 350 × 228 mm field of view; and a coronal T1-weighted sequence (500/21; echo train length, 4; matrix, 384 × 269) and a coronal fat-suppressed T2-weighted sequence (3570/72; echo train length, 10; matrix, 320 × 224), with a 3-mm section thickness, 0.6-mm intersection gap, and 350 × 350 mm field of view.

Image analysis

Two radiologists (reader 1, a radiologist with 9 years' experience in musculoskeletal radiology with experience in over 100 cases of material density images for evaluating bone marrow edema on DECT; reader 2, a resident-in-training radiologist with 9 months' experience in radiologic imaging and no experience in material density images on DECT) blind to the clinical data retrospectively evaluated DECT and MR images.

Qualitative analysis

Readers independently assessed the extent and severity of hip bone marrow edema in two different sessions: from water-HAP images in session 1 and from MR images in session 2. Reading sessions for the same patient were separated by at least 2 weeks to reduce recall bias.

In session 1, the axial water-HAP images were selected for determining the extent and severity of bone marrow edema. Coronal water-HAP images were analyzed as a supplement. Bone marrow edema of the proximal femur was analyzed for extent and severity. Edema extent scores were assigned as follows: grade 0, no edema; grade 1, edema in only femoral head; grade 2, edema in femoral head and neck; and grade 3, edema in femoral head, neck, and intertrochanter. Edema severity scores were qualitatively graded as follows: grade 0, no edema; grade 1, mild edema; grade 2, moderate edema; and grade 3, severe edema. Grades according to severity of edema in images are described in Fig. 2. The subcortical zone less than 4 mm from the cortical bone was excluded to minimize artifacts that might impede analysis. Although a previous study set the distance from the cortical zone as 2 mm with dual-energy virtual non-calcium imaging [11, 16], we set the standard distance at 4 mm as subcortical abrupt hyperdense artifacts seen at distances 3–4 mm from the cortex in the water-HAP image. We evaluated only the extent and severity of edema, except for any bone structural abnormalities.

In session 2, MR images were analyzed for the extent and severity of edema with the aforementioned grading systems on water-HAP images. MRI served as the reference standard. When both readers had different conclusions, the extent and severity grading on MRI was determined by consensus:

Consensus training was performed with 10 water-HAP and MR images to minimize inter-investigator variation.
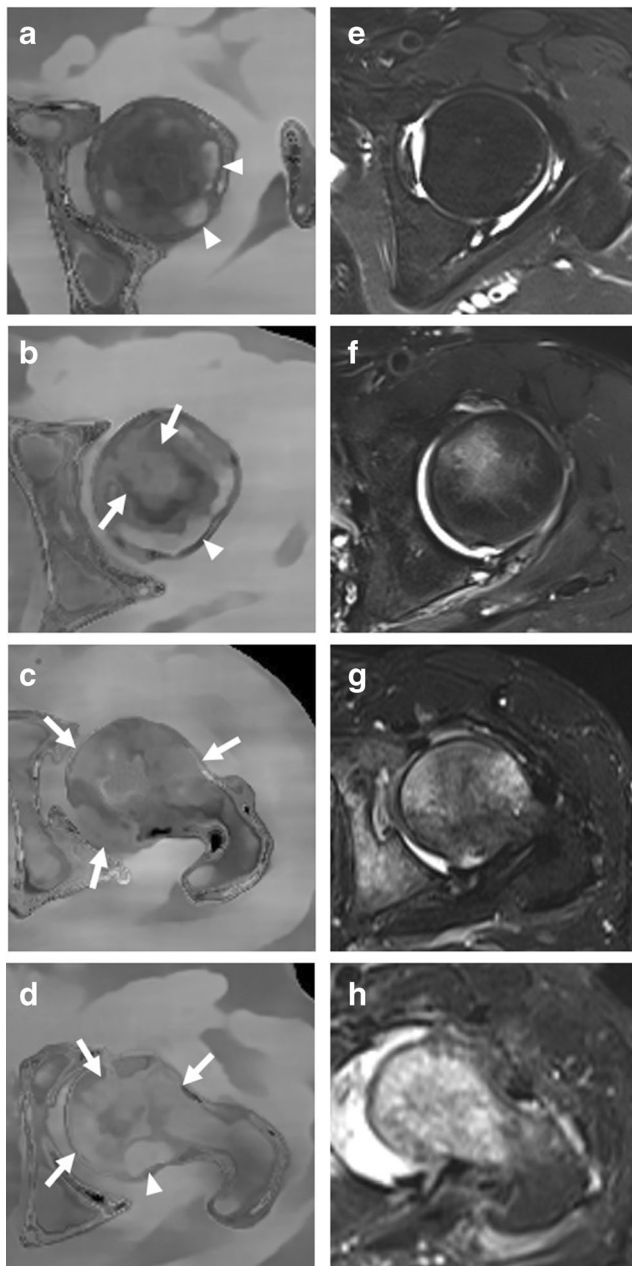
Fig. 2 Axial dual-energy water-HAP (**a**–**d**) and axial fat-suppressed T2-weighted MR (**e**–**h**) images showing no bone marrow edema (grade 0) in a 57-year-old female (**a**, **e**), mild edema (grade 1) in a 64-year-old female (arrow in **b**, **f**), moderate edema (grade 2) in a 57-year-old male (arrow in **c**, **g**), and severe edema (grade 3) in a 75-year-old female (arrow in **d**, **h**) patients. Subcortical zone less than 4 mm from the cortical bone was excluded from the analysis on water-HAP image to minimize subcortical abrupt hyperdense artifact (arrowhead in **a**, **b**, and **d**)

Subsequently, a grading system was used to determine the extent and severity of edema in hip joints.
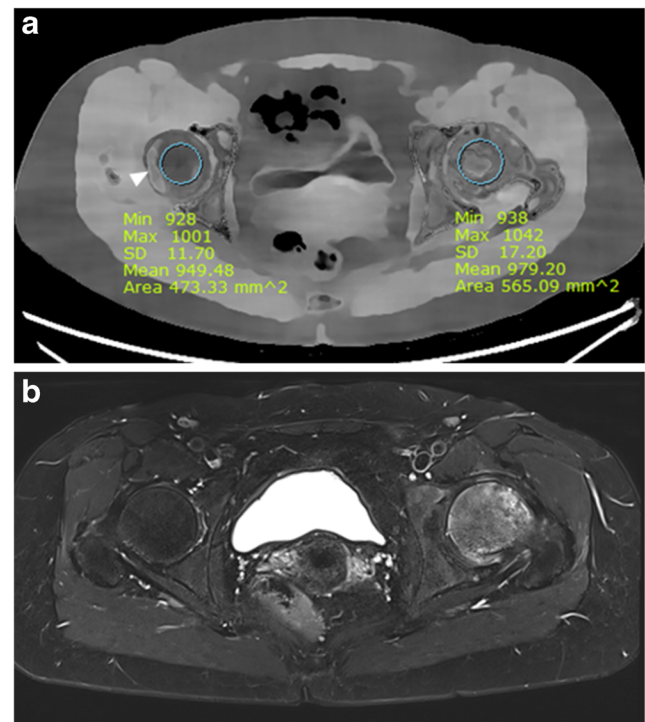
Quantitative analysis

After qualitative analyses were completed, readers independently measured mean water mass density using circular

regions of interest (ROIs) as the edema zone on axial water-HAP images, corresponding to the highest signal intensity of edema on axial T2-weighted MR images. ROI areas were maximized, and subcortical zones less than 4 mm or abnormal bone marrow lesions were excluded to reduce artifacts. If there was a unilateral edema at a hip joint, the same location of the contralateral hip joint was the ROI and if there was no edema in both hip joints, the mid-femoral head was the ROI (Fig. 3).

Statistical analysis

Sensitivity, specificity, accuracy, positive predictive value, and negative predictive value were calculated based on a contingency table with data from qualitative analysis of water-HAP images with reference to MRI for the presence of edema. McNemar's test and the kappa (κ) statistic were used to compare the presence of edema between readers 1 and 2.

Comparison of mean water mass density between areas with and without edema was analyzed by Student's t test and area depending on the extent and severity of edema by the

Fig. 3 Axial dual-energy water-HAP image (**a**) and axial fat-suppressed T2-weighted MR image (**b**) showing a 57-year-old female patient with a unilateral bone marrow edema of a left femoral head. Readers independently measured mean water mass density (mg/cm^3) using circular regions of interest as the edema zone of left femoral head on axial water-HAP image (**a**), corresponding to the highest signal intensity of bone marrow edema on MR image (**b**). Readers also placed regions of interest on the same location of the contralateral hip joint. Subcortical zone less than 4 mm from the cortical bone was excluded from the analysis on water-HAP image to minimize subcortical abrupt hyperdense artifact (arrowhead in **a**)

Mann-Whitney U test. For analysis, the extent and severity of edema were classified into two comparisons ("head" versus "head to neck + head to intertrochanter"; "mild" versus "moderate + severe"). Inter-reader agreement was determined using an interclass correlation coefficient (ICC) for water mass density value on water-HAP images. Receiver operating characteristic (ROC) curve analysis and calculation of the area under the ROC curve (AUROC) were used to evaluate the highest accuracy cutoff value of the water mass density on water-HAP images. Sensitivity, specificity, accuracy, and AUROC were calculated from the cutoff value.

Degrees of agreement based on ICCs and kappa values were interpreted using the following criteria: 0–0.20, poor; 0.21–0.40, fair; 0.41–0.60, moderate; 0.61–0.80, good; and 0.81–1.00, excellent [28]. P values < 0.05 were considered statistically significant. Statistical analyses were performed with SPSS (version 21.0; IBM).

Results

Forty consecutive patients enrolled in this study (mean age, 58 years [95% CI, 55; 61 years]; age range, 34–77 years): 16 men (mean age, 53 years [95% CI, 48; 58 years]; range, 34–69 years) and 24 women (mean age, 62 years [95% CI, 58; 66 years]; range, 41–77 years). Eighty hip joints were analyzed. Patient demographics are described in Table 1. The mean interval between DECT and MR imaging was 9 days (95% CI, 5; 13 days; range, 0–31 days).

Qualitative analysis

Reader 1 achieved overall sensitivity of 85%, specificity of 93%, accuracy of 89%, a positive predictive value of 92%, and a negative predictive value of 86%. The respective values for reader 2 were 85%, 73%, 79%, 76%, and 83% (Table 2, Fig. 4).

Reader 1 had 6 false-negative findings and 3 false-positive findings on water-HAP images for differentiation of the presence of edema from no edema. Reader 2 had 6 false-negative findings and 11 false-positive findings.

The McNemar test results show no significant difference between readers in the presence of edema in the hip joints (p = 0.077). Among 80 hip joints, readers disagreed with the presence of edema in water-HAP images on 16 joints. Inter-reader agreement for the presence of edema on water-HAP images was good (κ = 0.624, p < 0.001).

Quantitative analysis

Mean water mass density was significantly different regarding the presence (p < 0.017), extent ("head" versus "head to neck + head to intertrochanter," p < 0.003), and severity ("mild"

Table 1 Patients demographics

Characteristic	No.
Sex	
Male	16 (40)
Female	24 (60)
Pain	
Pain	49 (61)
No pain	31 (39)
Clinical diagnosis	
Normal	32 (40)
Osteonecrosis	25 (31)
Osteoarthritis	18 (23)
Others*	5 (6)
Extent of bone marrow edema at MRI	
No edema	40 (50)
Femoral head	18 (23)
Head to neck	4 (5)
Head to intertrochanter	18 (23)
Severity of bone marrow edema at MRI	
No edema	40 (50)
Mild	19 (24)
Moderate	18 (23)
Severe	3 (4)

Note: Data in parentheses are percentages and were calculated with a denominator of 40 patients or 80 joints. Others* includes hip synovitis (n = 2), transient bone edema syndrome (n = 1), impingement (n = 1), and Legg-Calve-Perthes sequelae (n = 1)

versus "moderate + severe," p < 0.035) of edema in water-HAP images (Table 3). ICC values between the readers for the value of water mass density were excellent (ICC = 0.885, p < 0.001).

The AUROC values were 0.96 for reader 1 and 0.91 for reader 2 in differentiating the presence of edema from no edema. The optimal water mass density to classify the presence of edema for reader 1 was 951 mg/cm^3 with a sensitivity

Table 2 Diagnostic performance of dual-energy water-HAP imaging in qualitative analysis according to the presence of bone marrow edema

Parameter	Reader 1	Reader 2
Sensitivity (%)	85 (75, 90) [34/40]	85 (74, 93) [34/40]
Specificity (%)	93 (82, 98) [37/40]	73 (61, 80) [29/40]
Accuracy (%)	89 (79, 94) [71/80]	79 (67, 87) [63/80]
PPV (%)	92 (81, 98) [34/37]	76 (66, 83) [34/45]
NPV (%)	86 (77, 91) [37/43]	83 (70, 92) [29/35]

Data are percentage. Data in parentheses are 95% confidence intervals, and data in brackets are the numerator and denominator. Inter-reader agreement for the presence of bone marrow edema on water-HAP images was good (κ = 0.624, p < 0.001). *HAP*, hydroxyapatite; *PPV*, positive predictive value; *NPV*, negative predictive value
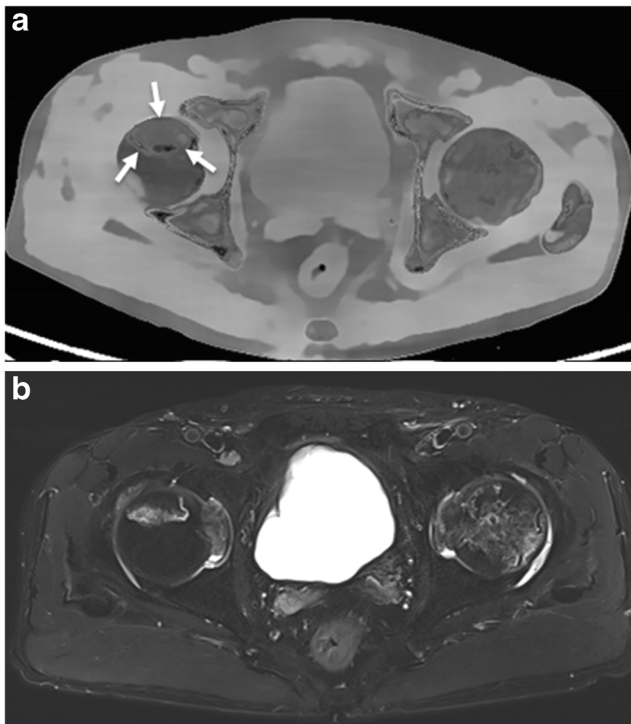
Fig. 4 Axial dual-energy water-HAP image (**a**) and axial fat-suppressed T2-weighted MR image (**b**) showing a 64-year-old male patient with both hip osteonecrosis and left femoral head bone marrow edema. Reader 1 interpreted the subcortical hyperdense lesion (arrow) of right anterior femoral head as structural abnormality of bone and analyzed as no bone marrow edema (grade 0) and reader 2 as mild bone marrow edema (grade 1). In the left femoral head, both readers analyzed the high density lesion as mild bone marrow edema (grade 1)

of 93% and a specificity of 93% and for reader 2, it was 957 mg/cm^3 with a sensitivity of 80% and a specificity of 80% (Table 4).

Discussion

Our study suggested that the diagnostic performance of dual-energy water-HAP imaging was effective at detecting bone marrow edema in non-traumatic hips. Measuring water mass density provides a satisfactory distinction between areas with and without edema. Furthermore, the more severe the edema, the higher was the mean water density value.

We evaluated bone marrow edema of non-traumatic hip diseases such as osteonecrosis and osteoarthritis. Most previous studies [12, 14–16, 19, 20, 22, 29] evaluated edema in patients with trauma or fracture by DECT. Diagnostic performances of detecting edema in these studies had 77–100% sensitivity and 40–100% specificity for acute knee trauma [16], traumatic ankles [19], vertebral fractures [14, 15, 22, 29], and hip fractures [12, 20]. Our quantitative analysis of non-traumatic hips showed that water-HAP images had 85% sensitivity and 93% specificity in reader 1 for detecting

edema. This is similar to the study that evaluated edema of sacroiliac joints in axial spondyloarthropathy (87% and 93% sensitivity and 94% and 91% specificity) [11]. Our study and an that of Wu H et al [11] have shown the possibility of applying DECT to non-traumatic disease. The diagnostic performance of edema detection using DECT showed a relatively wide range. Detecting edema may be related to the extent and severity of edema. Our study also showed that mean water mass density was significantly different according to the extent and severity of edema.

The diagnostic performance of qualitative analysis in our study showed relative differences between the readers (reader 1 vs. 2: sensitivity, 85% vs. 85%; specificity, 93% vs. 73%; accuracy, 89% vs. 79%; positive predictive value, 92% vs. 76%; negative predictive value, 86% vs. 83%). Osteonecrosis and osteoarthritis usually have combined structural bone changes including subchondral cystic change and sclerosis [2, 9, 13, 30–32]. These structural bone changes could be misinterpreted as edema in water-HAP imaging. The more experienced reader 1 might have differentiated structural bone change and edema better than reader 2 who had no experience in water-HAP imaging. Moreover, reader 2 was a resident-in-training radiologist with 9 months of experience in radiologic imaging. The mean radiologist's imaging experience in previous studies detecting bone marrow edema in DECT images was 8.9 years (range, 1–25 years) [11, 12, 14–16, 19, 20, 22, 29]. In addition, although we evaluated water-HAP images without conventional CT imaging to decrease bias, water-HAP imaging in detecting edema may be more useful with conventional CT imaging [15].

We acquired water-HAP images using two-material decomposition by single-source rapid kVp-switching DECT. Most previous studies [12, 14–16, 19–21] acquired virtual non-calcium images using three-material decomposition by dual-source DECT. The rapid kVp-switching method can obtain two sinogram data at the same projection angle and can efficiently perform beam-hardening correction using the two sinograms [17]. Ultimately, the beam-hardening free image preserves the original pixel values, resulting in more accurate material density values, which can be one advantage in the rapid kVp-switching method. The two-material decomposition algorithm assumes the X-ray projected object is composed of only two materials, and any two materials can be selected for clinical purposes. Similarly, the three-material decomposition algorithm assumes the object is made of three materials. In most previous studies [12, 14–16, 19–21], bone mineral, yellow marrow and red marrow were selected for evaluation of edema. The material density (mg/cm^3) of the pre-selected materials can be obtained with two-material decomposition algorithm. In our study, the mean cutoff value for discrimination between edema and non-edema was 951 mg/cm^3 with sensitivity and specificity of 93%, respectively. However, the three-material decomposition algorithm needs volume conservation to discriminate more than two materials.

Table 3 Water mass density at dual-energy water-HAP imaging according to the presence, extent, and severity of bone marrow edema

Parameter	Reader 1	p	Reader 2	p
Presence of bone marrow edema		0.001*		0.016*
No edema	941 (939, 943)		945 (941, 949)	
Edema	973 (968, 978)		975 (969, 981)	
Extent of bone marrow edema†		0.002		0.001
Femoral head	964 (957, 971)		963 (957, 969)	
Head to neck	982 (976, 988)		989 (975, 1003)	
Head to intertrochanter	979 (973, 985)		983 (975, 991)	
Severity of bone marrow edema†		0.003		0.034
Mild	965 (958, 972)		968 (960, 976)	
Moderate	977 (972, 982)		978 (970, 986)	
Severe	994 (986, 1002)		994 (985, 1003)	

Note.—Data are mean value of water mass density (mg/cm^3). Data in parentheses are 95% confidence intervals. *p values are calculated with t-test. †For analysis, extent and severity of bone marrow edema are classified into two comparisons ("head" versus "head to neck + head to intertrochanter"; "mild" versus "moderate + severe") and p values are calculated with Mann-Whitney test. $P < 0.05$ indicates a significant difference. ICC value between the readers are excellent (ICC = 0.885, $p < 0.001$). HAP = hydroxyapatite

The three-material decomposition algorithm provides gradient information such as the CT number (Hounsfield units) of each material, not density, because of the constraint of volume conservation. Although water-HAP imaging and virtual non-calcium imaging differ in data acquisition, material decomposition algorithms, and actual measured values, there are no studies comparing diagnostic performance in evaluating bone marrow between the two methods, and further studies are needed.

The mean volume CTDI of the previous DECT studies [11, 14–16, 19, 22, 29] assessing bone marrow edema was 11.6 mGy (range, 7.4–15.5 mGy), which is similar to our study (11.1 mGy). Two previous studies have compared the radiation dose of DECT with conventional CT for evaluating bone marrow lesions. Pache et al [16] reported that the CTDI of DECT was 28% higher compared to conventional CT (CTDI: DECT, 11.15 mGy; conventional CT, 8.71 mGy) and Guggenberger et al [19] reported that the CTDI of DECT was 1 mGy higher than conventional CT (CTDI: DECT, 15 mGy; conventional CT, 14 mGy). The radiation

Table 4 Diagnostic performance of dual-energy water-HAP imaging in quantitative measurement of water mass density

Parameter	Reader 1	Reader 2
Sensitivity (%)	93 (83, 97) [37/40]	80 (69, 88) [32/40]
Specificity (%)	93 (83, 97) [37/40]	80 (69, 88) [32/40]
Accuracy (%)	93 (83, 97) [74/80]	80 (69, 88) [64/80]
Area under the ROC curve	0.96	0.91
Cutoff value	951	957
p value	< 0.001	< 0.001

Data in parentheses are 95% confidence intervals, and data in brackets are the numerator and denominator. Data are the results of comparison between bone marrow edema and no edema. $P < 0.05$ indicates a significant difference. *ROC*, receiver operating characteristic; *HAP*, hydroxyapatite

dose of our study was acceptable in comparison with the other studies.

Our study had several limitations. First, the experienced reader had better diagnostic performance than the inexperienced reader. More readers will verify the relationship between diagnostic performance and experience in water-HAP imaging. Second, subcortical zones less than 4 mm could not be evaluated and were excluded to reduce artifacts. Third, we evaluated only water-HAP images without conventional CT images to minimize bias. If we evaluated images using both conventional and water-HAP images, it might have reduced false-positive findings due to structural bony abnormalities. Fourth, extent and severity of edema were classified into two comparisons due to small numbers of several subcategories.

In conclusion, dual-energy water-HAP imaging was considerably helpful for detection of bone marrow edema by using qualitative imaging evaluation and quantitative measurement of water mass density value in patients with non-traumatic hip pain. For higher diagnostic performance, radiologists should be experienced in reading water-HAP images.

Compliance with ethical standards

Guarantor The scientific guarantor of this publication is Chankue Park.

Conflict of interest The authors of this manuscript declare no relationships with any companies whose products or services may be related to the subject matter of the article.

Statistics and biometry One of the authors (Chankue Park) has significant statistical expertise.

Informed consent Written informed consent was waived by the Institutional Review Board.

Ethical approval Institutional Review Board approval was obtained.

Methodology
• Retrospective
• Observational
• Performed at one institution

References

1. Link TM, Steinbach LS, Ghosh S et al (2003) Osteoarthritis: MR imaging findings in different stages of disease and correlation with clinical findings. Radiology 226:373–381
2. Murphey MD, Foreman KL, Klassen-Fischer MK, Fox MG, Chung EM, Kransdorf MJ (2014) From the radiologic pathology archives imaging of osteonecrosis: radiologic-pathologic correlation. Radiographics 34:1003–1028
3. Kijowski R, Stanton P, Fine J, De Smet A (2006) Subchondral bone marrow edema in patients with degeneration of the articular cartilage of the knee joint. Radiology 238:943–949
4. Taljanovic MS, Graham AR, Benjamin JB et al (2008) Bone marrow edema pattern in advanced hip osteoarthritis: quantitative assessment with magnetic resonance imaging and correlation with clinical examination, radiographic findings, and histopathology. Skeletal Radiol 37:423–431
5. Felson DT, McLaughlin S, Goggins J et al (2003) Bone marrow edema and its relation to progression of knee osteoarthritis. Ann Intern Med 139:330–336
6. Iida S, Harada Y, Shimizu K et al (2000) Correlation between bone marrow edema and collapse of the femoral head in steroid-induced osteonecrosis. AJR Am J Roentgenol 174:735–743
7. Ito H, Matsuno T, Minami A (2006) Relationship between bone marrow edema and development of symptoms in patients with osteonecrosis of the femoral head. AJR Am J Roentgenol 186:1761–1770
8. Ragab Y, Emad Y, Abou-Zeid A (2008) Bone marrow edema syndromes of the hip: MRI features in different hip disorders. Clin Rheumatol 27:475–482
9. Mallinson PI, Coupal TM, McLaughlin PD, Nicolaou S, Munk PL, Ouellette HA (2016) Dual-energy CT for the musculoskeletal system. Radiology 281:690–707
10. Booz C, Nöske J, Martin SS et al (2018) Virtual noncalcium dual-energy CT: detection of lumbar disk herniation in comparison with standard gray-scale CT. Radiology 290:446–455
11. Wu H, Zhang G, Shi L et al (2018) Axial spondyloarthritis: dual-energy virtual noncalcium CT in the detection of bone marrow edema in the sacroiliac joints. Radiology 290:157–164
12. Kellock TT, Nicolaou S, Kim SS et al (2017) Detection of bone marrow edema in nondisplaced hip fractures: utility of a virtual noncalcium dual-energy CT application. Radiology 284:798–805
13. Stevens K, Tao C, Lee S-U et al (2003) Subchondral fractures in osteonecrosis of the femoral head: comparison of radiography, CT, and MR imaging. AJR Am J Roentgenol 180:363–368
14. Wang CK, Tsai JM, Chuang MT, Wang MT, Huang KY, Lin RM (2013) Bone marrow edema in vertebral compression fractures: detection with dual-energy CT. Radiology 269:525–533
15. Kaup M, Wichmann JL, Scholtz JE et al (2016) Dual-energy CT–based display of bone marrow edema in osteoporotic vertebral compression fractures: impact on diagnostic accuracy of radiologists with varying levels of experience in correlation to MR imaging. Radiology 280:510–519
16. Pache G, Krauss B, Strohm P et al (2010) Dual-energy CT virtual noncalcium technique: detecting posttraumatic bone marrow lesions—feasibility study. Radiology 256:617–624
17. Patino M, Prochowski A, Agrawal MD et al (2016) Material separation using dual-energy CT: current and emerging applications. Radiographics 36:1087–1105
18. Mendonça PR, Lamb P, Sahani DV (2013) A flexible method for multi-material decomposition of dual-energy CT images. IEEE Trans Med Imaging 33:99–116
19. Guggenberger R, Gnannt R, Hodler J et al (2012) Diagnostic performance of dual-energy CT for the detection of traumatic bone marrow lesions in the ankle: comparison with MR imaging. Radiology 264:164–173
20. Reddy T, McLaughlin P, Mallinson P et al (2015) Detection of occult, undisplaced hip fractures with a dual-energy CT algorithm targeted to detection of bone marrow edema. Emerg Radiol 22:25–29
21. Kosmala A, Weng AM, Krauss B, Knop S, Bley TA, Petritsch B (2018) Dual-energy CT of the bone marrow in multiple myeloma: diagnostic accuracy for quantitative differentiation of infiltration patterns. Eur Radiol 28:5083–5090
22. Akisato K, Nishihara R, Okazaki H et al (2019) Dual-energy CT of material decomposition analysis for detection with bone marrow edema in patients with vertebral compression fractures. Acad Radiol
23. Kumar V, Abbas AK, Aster JC (2014) Robbins and Cotran pathologic basis of disease, 9th edn. Elsevier, Philadelphia
24. Gartner LP, Hiatt JL (2013) Color atlas and text of histology, 6th edn. Lippincott Williams & Wilkins, Baltimore Philadelphia
25. Ai S, Qu M, Glazebrook KN et al (2014) Use of dual-energy CT and virtual non-calcium techniques to evaluate post-traumatic bone bruises in knees in the subacute setting. Skeletal Radiol 43:1289–1295
26. International Commission on Radiation Units and Measurements (1992) Photon, electron, proton and neutron interaction data for body tissues (ICRU–46). Bethesda, MD
27. Hubbell JH, Seltzer SM (1995) Tables of X-ray mass attenuation coefficients and mass energy-absorption coefficients 1 keV to 20 MeV for elements Z = 1 to 92 and 48 additional substances of dosimetric interest. National Inst. of Standards and Technology - Ionizing Radiation Division. Gaithersburg, MD
28. Landis JR, Koch GG (1977) The measurement of observer agreement for categorical data. Biometrics 33:159–174
29. Diekhoff T, Hermann K, Pumberger M, Hamm B, Putzier M, Fuchs M (2017) Dual-energy CT virtual non-calcium technique for detection of bone marrow edema in patients with vertebral fractures: a prospective feasibility study on a single-source volume CT scanner. Eur J Radiol 87:59–65
30. Karachalios T, Karantanas AH, Malizos K (2007) Hip osteoarthritis: what the radiologist wants to know. Eur J Radiol 63:36–48
31. Koo K-H, Mont MA, Jones LC (2014) Osteonecrosis. Springer, Berlin Heidelberg
32. Malizos KN, Karantanas AH, Varitimidis SE, Dailiana ZH, Bargiotas K, Maris T (2007) Osteonecrosis of the femoral head: etiology, imaging and treatment. Eur J Radiol 63:16–28